

An Electronically 1-Bit Reconfigurable Beam-Steering Reflectarray Antenna of 12×12 Units Integrated with PIN Diodes

Weixiong Luo, Shixing Yu, Na Kou*, Zhao Ding, and Zhengping Zhang

Abstract—An electronically reconfigurable reflectarray antenna of 12×12 units is presented in this paper. The element consists of a slotted square patch and a gapped metal square ring. PIN diodes are loaded on slotted square patches, which can be electronically controlled to produce two states with 180° phase difference. A reflectarray prototype is fabricated and experimentally studied. Experimental results agree well with the full-wave simulations by Ansys HFSS, and scanning beams within $\pm 45^\circ$ range are obtained with a maximum aperture efficiency of 14.9% at 5.8 GHz. 1-dB bandwidth is 9.9%, and 3-dB bandwidth is 19.1%.

1. INTRODUCTION

Microstrip planar reflectarray antennas [1] can produce focused, shaped, or contoured beams by introducing sufficient phase shift in specific techniques (such as changing size of elements, introducing phase extension lines, and rotating units) [2, 3]. It has been verified that reflectarray antennas are compatible with the main advantages of parabolic reflectors and conventional phased arrays. Reconfigurable reflectarray antenna (RRA) elements differ from phased arrays because they do not require extra phase shifters and costly transmit/receive (T/R) modules. Only electronic switches, varactors, or tunable materials need to be introduced on the reflective elements [4]. In addition, because of the spatial feeding mechanism, the loss brought by the feeding network is avoided. Compared with phased arrays, reconfigurable reflectarray antennas have the advantages of low lossy, low cost, and high efficiency, and at the same time, they can also provide beam-scanning. In the future, it has the potential to be an alternative to expensive phased arrays [5, 6]. Currently applications based on PIN diodes for reconfigurable reflectarray are popular. Yang et al. come up with a simple 1-bit reconfigurable reflectarray and the experimental results get good agreements with his assumption in 2016 [7]. Furthermore, the stacked microstrip structure and a 1-bit microstrip line-slot phase shifter were introduced in [8] to achieve the wideband and reconfigurable characteristics. A wideband and low loss 1-bit RRA element was designed which consists of double-layer patches printed on two dielectric substrates, forming a multi-resonance behavior for expanding the bandwidth [9].

More and more reconfigurable reflectarrays are proposed and used in various scenarios. On the basis of previous work, this paper proposes and optimizes a simple broadband RAA unit at 5.8 GHz, and a prototype of RRA with 12×12 units is fabricated and measured. The proposed RRA can be applied in wireless communication in the future.

2. DESIGN OF THE ELEMENT

The topological structure of the designed electronically reconfigurable element is illustrated in Fig. 1. It consists of two metal layers and two dielectric layers. The upper metal layer consists of a gapped

Received 5 March 2022, Accepted 18 April 2022, Scheduled 29 April 2022

* Corresponding author: Na Kou (nkou@gzu.edu.cn).

The authors are with the Key Laboratory of Micro-Nano-Electronics and Software Technology of Guizhou Province, College of Big Data and Information Engineering, Guizhou University, Guiyang 550025, China.

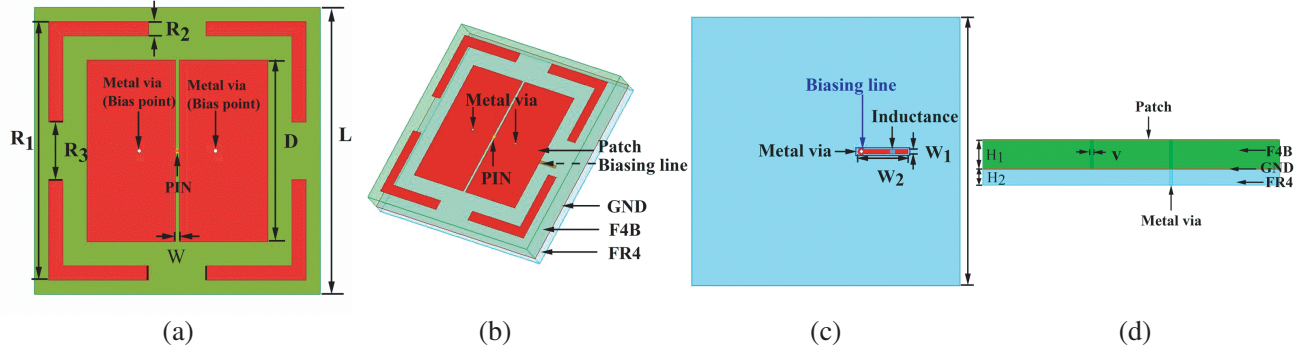


Figure 1. Cell topology. (a) Top view of the element. (b) Perspective view. (c) Bottom view. (d) Side view. ($L = 29$ mm, $R1 = 28$ mm, $R2 = 1$ mm, $R3 = 5$ mm, $D = 19.5$ mm, $W = 0.42$ mm, $V = 0.4$ mm, $W1 = 0.5$ mm, $W2 = 5$ mm, $H1 = 1.2$ mm, $H2 = 3$ mm).

square ring and a slotted square patch. The slotted patches are welded with a PIN diode. When the direct-current (DC) bias voltage is turned on or off, the PIN diode can result in a 180° phase difference by changing the resonance characteristics. Additionally, the DC bias network is placed on the backside of the bottom layer. Two bias points are located at the non-radiative edge of the patch. One of the bias points is connected to the bias network of the underlying dielectric (FR4) through metal via. The other bias point is connected to the ground through a metal via. In the bias network, welding inductors for suppressing radio-frequency (RF) signals can ensure good isolation of direct current and RF signals and reduce additional losses caused by the bias network.

We choose the Skyworks SMP1340-040LF as the PIN diode. According to the data sheet, it covers the required frequency band of 500 MHz–10 GHz and shows low insertion loss. For the wireless communication system at 5.8 GHz, its frequency band can be perfectly covered. The cell is modeled and simulated under infinite boundary condition in combination with Floquet port excitation by the electromagnetic simulators. In simulations, the PIN diode of SMP1340-040L is modeled in the simulator as an RLC boundary: $R = 1$ ohm and $L = 450$ pH in series for ON state, $R = 10$ ohm, $L = 450$ pH, and $C = 0.16$ pF in series for OFF state.

Full-wave simulation model of the reflectarray element is shown in Fig. 2(a). When the PIN diode

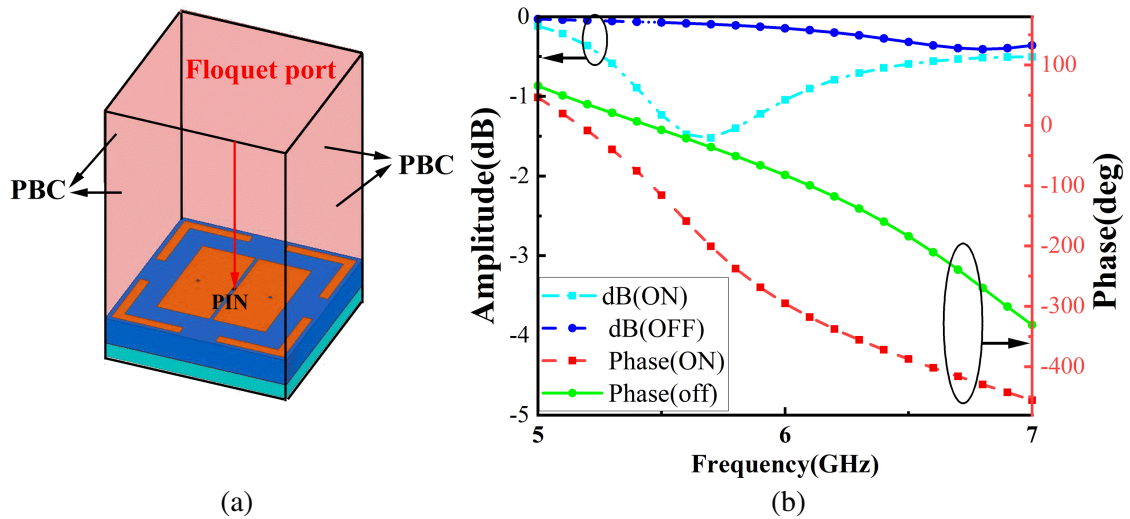


Figure 2. (a) Full-wave simulation model of the reflectarray element. (b) Simulated reflection amplitude and phase.

is turned on or off, it can be clearly observed that the reflection phase of this element is -230° and -50° at 5.8 GHz, respectively. As expected, the reflected phase difference between the two states remains a stable 180° in the desired frequency band by switching bias voltage. Additionally, reflection losses in the corresponding frequency band are less than 1.8 dB regardless of PIN status, as shown in Fig. 2(b).

3. RAA DESIGN AND ITS PHASE CONTROL BOARD

For experimental verification, a prototype of electronically reconfigurable reflectarray with 12×12 elements was designed, fabricated, and measured as shown in Fig. 3. The aperture size is $375 \text{ mm} \times 375 \text{ mm}$. A horn is used as the primary feed to generate y -polarized incident waves of 30° . The F/D ratio is 0.92. The center of the horn antenna is in parallel with the edge of the reflectarray, and the distance between the horn antenna and the edge of array is 330 mm. The 3D printer prints the bracket in order to assemble the array and phase control board together, which is convenient for testing.

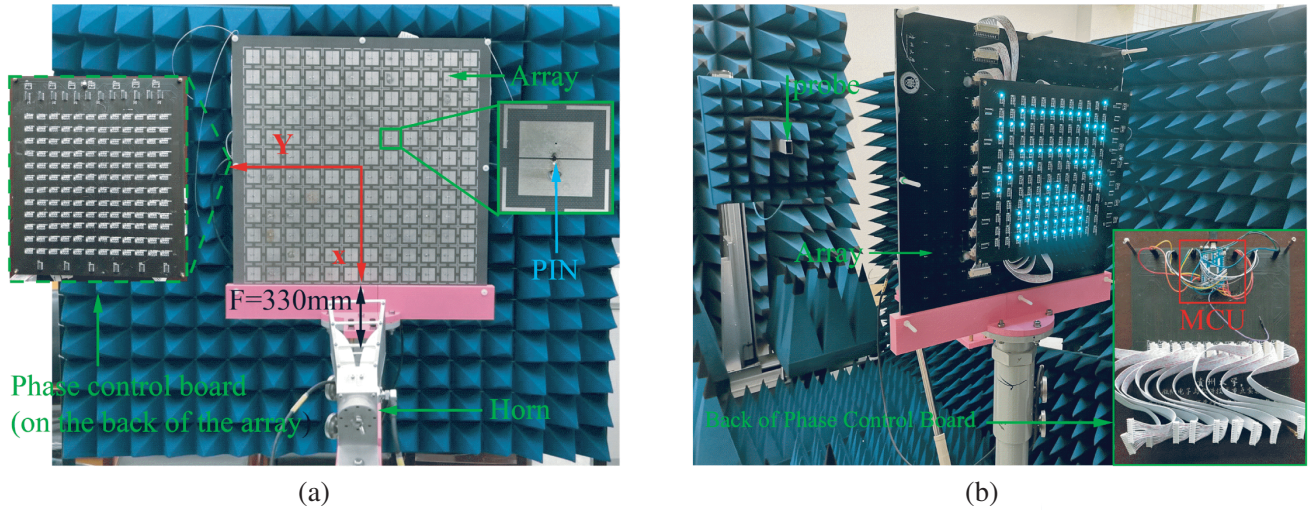


Figure 3. (a) Top view of fabricated reflectarray antenna. (b) Side view of fabricated reflectarray antenna.

The control board is an integral part of the RRA design. It controls the DC bias voltage on each PIN diode based on the difference in compensation phase, enabling electronic reconfigurability. The design idea of the phase control board is shown in Fig. 4(a), and the physical map is reflected in Fig. 3. The main system uses a microcontroller unit (MCU) that distributes control data to 18 shift registers in parallel and is synchronized with a clock (CLK) signal. In the data sheet of PIN diodes (SMP1340-040LF), it states that the diode turn-on voltage is 0.5 V–0.8 V. To obtain the required turn-on voltage, the output of the shift register (MCU output voltage is 5 V) should be connected to a voltage divider resistor, so that the line connected to the diode can obtain a turn-on voltage of 0.5 V–0.8 V. Finally, a feedback mechanism is set up with an LED in series with each PIN diode to indicate the PIN status. This makes the debugging and testing process easier.

By using lumped elements to dynamically adjust the phase shift of all reflective elements independently, a beam-scannable reflective array can be realized. To control the reflected beam, the phase shift ϕ_{mn} should be determined. Due to the different distances from the feed to each unit, the path delays need to be compensated when the feed horn irradiates the reflectarray. The compensated phase shift for each reflectarray element consists of two parts: the path delay of the feed horn antenna and the required phase shift for beam deflection [1]. For a reflectarray antenna, the required compensation phase-shift can be calculated as follows [7]:

$$\phi_{mn} = k_0(d_{mn} - (x_{mn} \cos \varphi_0 + y_{mn} \sin \theta_0)) \quad (1)$$

where ϕ_{mn} is the compensated phase required by the (m,n) -th unit cell of the reflectarray. k_0 presents the wave number in a vacuum. d_{mn} indicates the distance from the center point of the (m,n) -th element from the array to the feed horn. (θ_0, φ_0) is the beam direction. We quantify the phase shift as follows [10]:

$$\phi_{mn}^q = \begin{cases} 0, & -\pi/2 < \phi_{mn} < \pi/2 \\ \pi, & \pi/2 < \phi_{mn} < \pi \quad \text{and} \quad -\pi < \phi_{mn} < -\pi/2 \end{cases} \quad (2)$$

where ϕ_{mn} is the compensated phase required by the (m,n) -th unit cell of the reflectarray, and ϕ_{mn}^q denotes the 1-bit quantized phase. The phase quantization diagram of 0° is shown in Fig. 4(b).

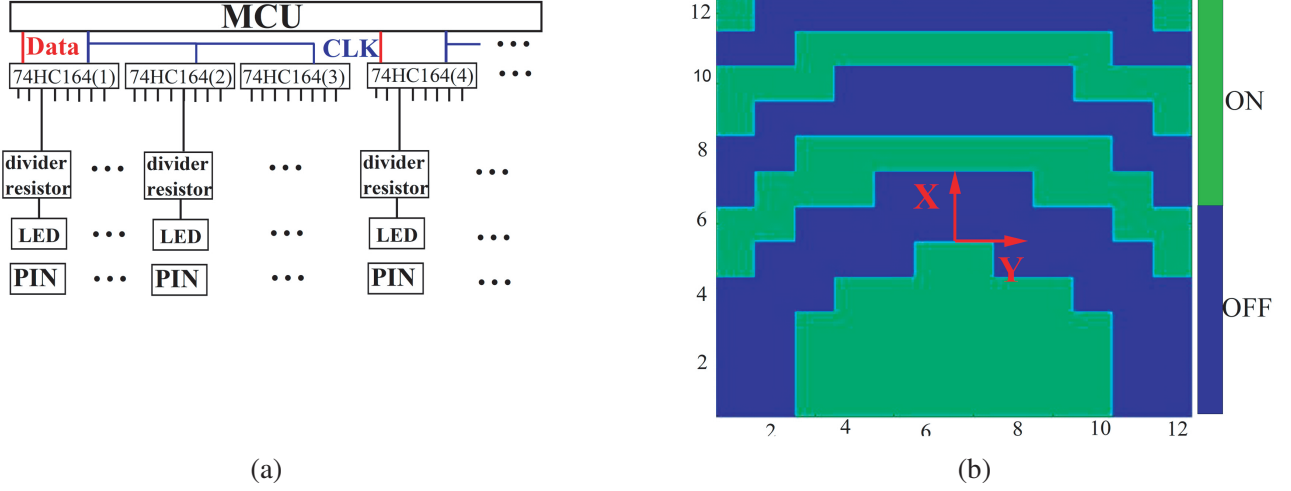


Figure 4. (a) Block diagram of the phase control board. (b) Quantized phase distribution for generating beam at $\theta = 0^\circ$.

4. BEAM-SCANNING PERFORMANCE

The phase compensation of the RRA can be controlled by changing the state of the PIN diode, resulting in an electronically scanned beam. Fig. 5(a) shows the beam scanning results measured on the yo z plane at 5.8 GHz. It can be seen that good beam scanning performance is obtained in the $\pm 45^\circ$ elevation

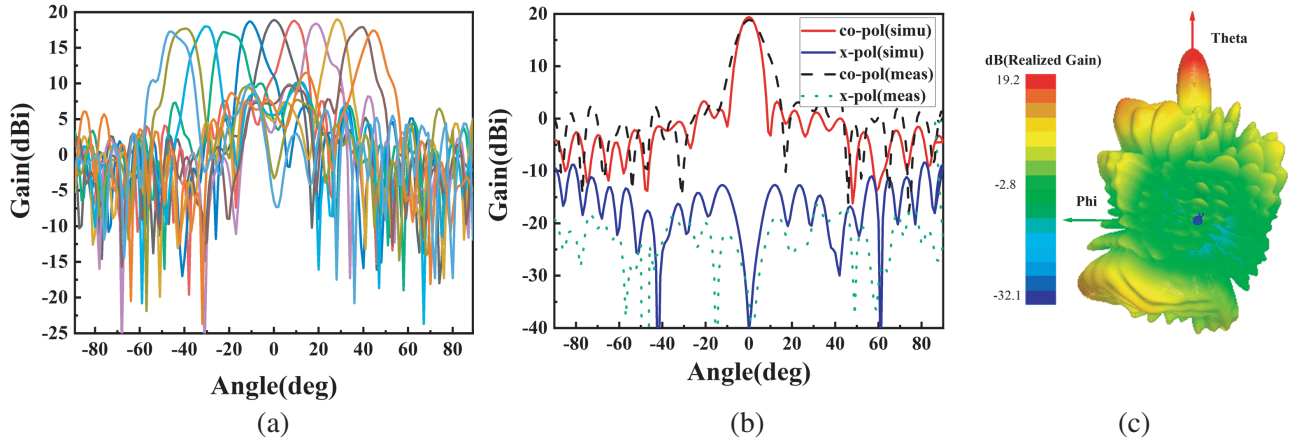


Figure 5. (a) Beam-scanning of the yo z plane. (b) Comparisons of simulated and measured radiation patterns at 5.8 GHz. (c) 3D radiation patterns of reflectarray antenna when beam direction is at $(\theta_0, \varphi_0) = (0^\circ, 0^\circ)$.

angle range. The average sidelobe level is less than -8 dB. The RRA prototype can successfully obtain the scanning beams. From measured radiation patterns we can see that the half-power beamwidth increases with scanning angle. When the scanning angle is 0° and 50° , the angles are about 9° and 20° . In addition, the gain decreases when scanning angle becomes large. Since the incident wave of the feed horn irradiates the array at 30° , a parasitical beam appears in the direction of the ϕ angle, as shown in Fig. 5(c). Simulated and measured radiation patterns in the yoz plane at 5.8 GHz are shown in Fig. 5(b). The measured cross-polarization performance is also shown in Fig. 5(b). The measured cross-polarization level is 30 dB lower than co-polarization. The measured gain is 18.9 dBi. According to formula (3):

$$\eta = \frac{G\lambda^2}{4\pi A} \quad (3)$$

where G is the measured gain, and A is the aperture area. We can calculate the aperture efficiency of 14.9%. Considering the quantization loss of a typical 1-bit RRA of about 3 dB, the theoretical aperture efficiency is expected to be 30%. The simulated and measured gains at different scanning angles are shown in Fig. 6(a). The bandwidth performance of RAA was measured. As shown in Fig. 6(b), the agreement between simulation and measurement is good, and the gain is stable in the frequency band of interest. 1-dB bandwidth is 9.9%, and 3-dB bandwidth is 19.1%. It is worth mentioning that we list other works in Table 1 and find that the 3-dB bandwidth of 19.1% is the best. In this paper, we use the single-layer of dielectric substrate to design the reflectarray and achieve the 3-dB bandwidth of 19.1%. The proposed reflectarray antenna design has the advantages of wideband and low cost. However, this design has a problem of relatively low aperture efficiency which can be attributed to phase errors raised

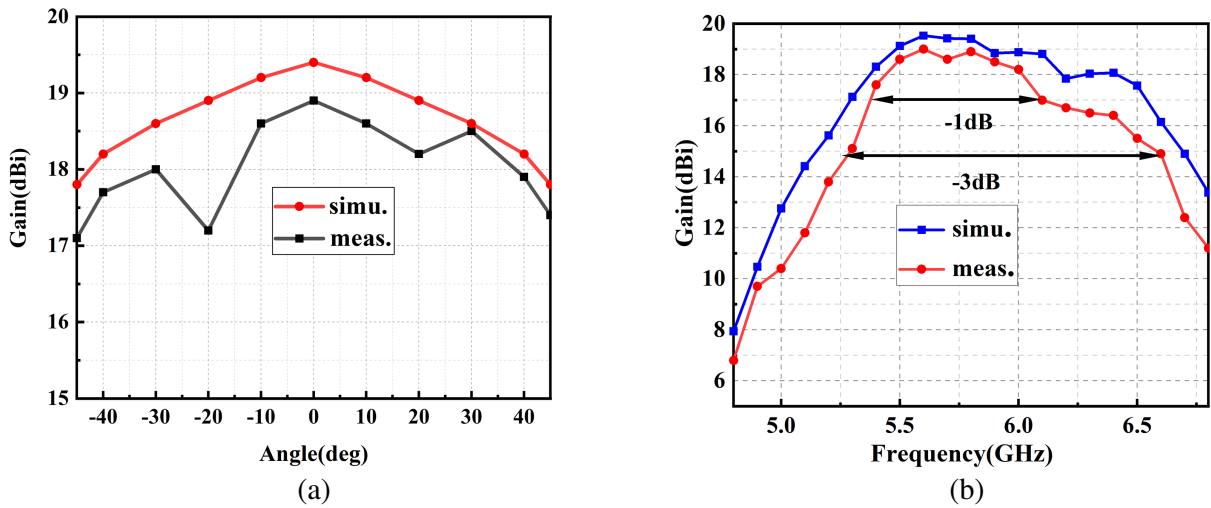


Figure 6. (a) Simulated and measured gains at different scan angles. (b) Comparison of simulated and measured gain bandwidth.

Table 1. Some works comparisons.

Ref.	[11]	[12]	[13]	[14]	This work
Frequency (GHz)	5	12.5	5.4	11	5.8
Phase control method	PIN	PIN	Varactor diode	Varactor diode	PIN
Phase shift of the element	200°	180°	373°	318°	180°
Aperture efficiency (%)	15.26	13.2	-	18.3	14.9
1-dB bandwidth (%)	8.4	-	-	10	9.9
3-dB bandwidth (%)	-	17	3.6	-	19.1
Scanning Range (deg)	$\pm 50^\circ$	$\pm 60^\circ$	$\pm 40^\circ$	$\pm 50^\circ$	$\pm 45^\circ$

by quantization and measurement environment. This reconfigurable reflectarray antenna can be applied in 5G mobile communication and satellite communication systems.

5. CONCLUSION

In this paper, a reconfigurable reflectarray unit loaded with PIN diodes is designed. The simulation verification is carried out to ensure the accuracy of the design and provide a guarantee for the effectiveness of the reflectarray design. We design a phase control board of 144 parallel circuit signals and add LED light arrays corresponding to one-to-one on the reflectarray to observe the working states of each diode in real-time. A reconfigurable reflectarray is designed and fabricated with the proposed unit. The results show that the 1-bit reconfigurable reflectarray antenna can achieve adaptive beam scanning within a certain range, and the measured results are in good agreement with the simulated ones. Beam steering can be realized at the range of $\pm 45^\circ$. The gain is 18.9 dBi, and the scanning loss is within 2.5 dB, ensuring good beam scanning performance. Finally, the 1-dB bandwidth is 9.9%, and the 3-dB bandwidth is 19.1%.

ACKNOWLEDGMENT

This work was supported by the National Natural Science Foundation of China under Grant No. 61961006 and the Science and Technology Foundation of Guizhou Province under Grant No. QKHJC [2020]1Y256.

REFERENCES

1. Berry, D., R. Malech, and W. Kennedy, "The reflectarray antenna," *IEEE Transactions on Antennas and Propagation*, Vol. 11, No. 6, 645–651, 1963.
2. Li, Y. and A. Abbosh, "Reconfigurable reflectarray antenna using single-layer radiator controlled by PIN diodes," *IET Microw. Antennas Propag.*, Vol. 9, 664–671, 2015.
3. Perruisseau-Carrier, Julien and A. K. Skrivervik, "Monolithic mems-based reflectarray cell digitally reconfigurable over a 360° phase range," *IEEE Transactions on Antennas and Propagation*, Vol. 69, No. 9, 5585–5595, Sept. 2021.
4. Wu, F., R. Lu, J. Wang, Z. H. Jiang, W. Hong, and K.-M. Luk, "A circularly polarized 1 Bit electronically reconfigurable reflectarray based on electromagnetic element rotation," *IEEE Transactions on Antennas and Propagation*, Vol. 69, No. 9, 5585–5595, Sept. 2021.
5. Baracco, J.-M., P. Ratajczak, P. Brachat, J.-M. Fargeas, and G. Toso, "Ka-band reconfigurable reflectarrays using varactor technology for space applications: A proposed design," *IEEE Antennas and Propagation Magazine*, Vol. 64, No. 1, 27–38, Feb. 2022.
6. Pan, X., F. Yang, S. Xu, and M. Li, "A 10 240-element reconfigurable reflectarray with fast steerable monopulse patterns," *IEEE Transactions on Antennas and Propagation*, Vol. 69, No. 1, 173–181, Jan. 2021.
7. Yang, H., et al., "A 1-Bit 10×10 reconfigurable reflectarray antenna: Design, optimization, and experiment," *IEEE Transactions on Antennas and Propagation* Vol. 64, No. 6, 2246–2254, Jun. 2016.
8. Xi, B., Y. Xiao, K. Zhu, Y. Liu, H. Sun, and Z. Chen, "1-Bit wideband reconfigurable reflectarray design in Ku-band," *IEEE Access*, Vol. 10, 4340–4348, 2022.
9. Zhou, S.-G., et al., "A wideband 1-Bit reconfigurable reflectarray antenna at Ku-band," *IEEE Antennas and Wireless Propagation Letters*, Vol. 21, No. 3, 566–570, Mar. 2022.
10. Yu, S., L. Li, and N. Kou, "One-bit digital coding broadband reflectarray based on fuzzy phase control," *IEEE Antennas and Wireless Propagation Letters*, Vol. 16, 1524–1527, 2017.
11. Han, J., L. Li, G. Liu, Z. Wu, and Y. Shi, "A wideband 1 bit 12×12 reconfigurable beam-scanning reflectarray: Design, fabrication, and measurement," *IEEE Antennas and Wireless Propagation Letters*, Vol. 18, No. 6, 1268–1272, 2019.

12. Wang, Z., et al., "1 Bit electronically reconfigurable folded reflectarray antenna based on p-i-n diodes for wide-angle beam-scanning applications," *IEEE Transactions on Antennas and Propagation*, Vol. 68, No. 9, 6806–6810, Sept. 2020.
13. Riel, M. and J.-J. Laurin, "Design of an electronically beam scanning reflectarray using aperture-Coupled elements," *IEEE Transactions on Antennas and Propagation*, Vol. 55, No. 5, 1260–1266, 2007.
14. Costanzo, S., F. Venneri, A. Raffo, and G. Di Massa, "Dual-layer single-varactor driven reflectarray cell for broad-band beam-steering and frequency tunable applications," *IEEE Access*, Vol. 6, 71793–71800, 2018.